Microfluidic device for generating a stepwise concentration gradient on a microwell slide for cell analysis

Emilie Weibull,[1] Shunsuke Matsui,[2] Manabu Sakai,[2]
Helene Andersson Svahn,[1,a)] and Toshiro Ohashi[3]
[1]*Division of Proteomics and Nanobiotechnology, Science for Life Laboratory, KTH-Royal Institute of Technology, 171 65 Stockholm, Sweden*
[2]*Graduate School of Engineering, Hokkaido University, Sapporo, Hokkaido 060-8628, Japan*
[3]*Faculty of Engineering, Hokkaido University, Sapporo Hokkaido 060-8628, Japan*

(Received 22 October 2013; accepted 28 November 2013; published online 10 December 2013)

Understanding biomolecular gradients and their role in biological processes is essential for fully comprehending the underlying mechanisms of cells in living tissue. Conventional *in vitro* gradient-generating methods are unpredictable and difficult to characterize, owing to temporal and spatial fluctuations. The field of microfluidics enables complex user-defined gradients to be generated based on a detailed understanding of fluidic behavior at the μm-scale. By using microfluidic gradients created by flow, it is possible to develop rapid and dynamic stepwise concentration gradients. However, cells exposed to stepwise gradients can be perturbed by signals from neighboring cells exposed to another concentration. Hence, there is a need for a device that generates a stepwise gradient at discrete and isolated locations. Here, we present a microfluidic device for generating a stepwise concentration gradient, which utilizes a microwell slide's pre-defined compartmentalized structure to physically separate different reagent concentrations. The gradient was generated due to flow resistance in the microchannel configuration of the device, which was designed using hydraulic analogy and theoretically verified by computational fluidic dynamics simulations. The device had two reagent channels and two dilutant channels, leading to eight chambers, each containing 4 microwells. A dose-dependency assay was performed using bovine aortic endothelial cells treated with saponin. High reproducibility between experiments was confirmed by evaluating the number of living cells in a live-dead assay. Our device generates a fully mixed fluid profile using a simple microchannel configuration and could be used in various gradient studies, e.g., screening for cytostatics or antibiotics. © *2013 AIP Publishing LLC*.
[http://dx.doi.org/10.1063/1.4846435]

I. INTRODUCTION

Biomolecular gradients are known to play an essential role in a wide range of intra- and extra-cellular biological processes, including cell proliferation, immune responses, wound healing, and cancer.[1] Several *in vitro* methods, whereby cells are exposed to chemical gradients, have been developed to study the biological relevance of *in vivo* gradients. However, the traditional *in vitro* gradient-generating methods, e.g., Boyden chamber,[2] Zigmond chamber,[3] biological hydrogels,[4] and micropipette-based assay,[5] all depend on diffusion over time to create a gradient. Traditional methods have been invaluable for determining the mechanisms behind gradient-dependent cell responses elicited by newly identified biomolecules.[1] However, in free

a)Author to whom correspondence should be addressed. Electronic mail: helene.andersson.svahn@scilifelab.se. Tel./Fax: +46 8-52480096

solution, molecular diffusion is unrestricted and isotropic. This lack of restriction makes it difficult to quantify and characterize chemical gradients and the response they elicit, owing to temporal and spatial fluctuations. To decipher the in-depth characteristics of biomolecular gradients and how gradient dynamics are integrated to produce a specific cell response, a highly controlled user-defined profile is required.

Developments in the field of microfluidics have enabled the generation of readily quantifiable, reproducible, and predicable *in vitro* gradients.[1] A detailed understanding of the behavior of fluids at the μm-scale and accurate fabrication methods make microfluidics well suited for creating complex user-defined gradient environments that allow for both spatial and temporal control.

Two different approaches for generating gradients using microfluidics have been developed: Diffusion-based and flow-based microfluidic gradient devices.[6] In diffusion-based devices, gradients are generated by pure diffusion through a hydrogel or membrane. A disadvantage with diffusion-based gradients is the incapacity to generate dynamic gradient profiles. Flow-based devices allow control of concentration gradients through laminar flow with active or diffusive mixing, enabling gradients to be formed rapidly and dynamically. There are two categories of flow-based gradients. The first is continuous concentration gradients, which depend on diffusive mixing during flow to generate gradients[7] and can be used for chemotaxis and migration studies.[8,9] The second is stepwise concentration gradients. These gradients are usually generated using a ladder-type network of microchannels or by simple serial dilution, establishing numerous concentrations that enter the cell culture chamber, creating a gradient under continuous flow.[10,11] Stepwise concentration gradients can generate both a linear and logarithmic dilution series. The complex design principles are often based on the analogous behavior of hydraulic and electric circuits.[12]

Although stepwise concentration generators can be used to investigate cellular behavior induced by different concentrations, a precise analysis of the sensitivity of cells to specific chemicals is difficult to perform if the cells are contained in a single chamber. The behavior of cells exposed to a certain concentration may be affected by intercellular paracrine signaling, originating from neighboring cells exposed to a different concentration.[10] Therefore, there is a demand for devices that can create concentration steps of a certain reagent in discrete and isolated locations on a miniature scale. The approach has been employed in an apoptosis study, creating a gradient by opening and closing valves, which effectively separated the culture chambers[13] and in a coculture study, where a ladder-type network generated a gradient in five discrete culture chambers.[14]

We have previously developed a microwell slide for cellular analysis,[15] which consisted of an array of (14×48) microwells that could accommodate up to 672 single cells for cultivation over several weeks. The microwell slide was used to perform heterogeneity analysis on clonal expansion from single carcinoma cells,[16] culture and clonal assays of stem cells,[17] and polymerase chain reaction (PCR) amplifications and minisequencing.[18] In a previous paper, we showed that it was possible to integrate the microwell slide with microfluidic channels to facilitate liquid handling and enhance single cell analysis.[19] This device provided a high-throughput, reliable, and rapid method for observing variations in cell response.

In the present study, a microfluidic stepwise concentration gradient generator was developed and integrated to the microwell slide. The stepwise concentration gradient generator was designed to utilize the slides' compartmentalized structure to deliver precisely controlled flow volumes of a reagent and dilutant, generating eight discrete steps of reagent concentration in designated microwells. The microchannel configuration was designed by analogy with electrical and hydraulic circuits. Computational fluid dynamics (CFD) simulations were performed to theoretically verify the stepwise concentration gradient. A dose-dependency analysis study of the microwell device showed that cells in the eight individual microwell-chambers were subjected to a single concentration, eliminating problems associated with intercellular paracrine signaling from neighboring cells exposed to different concentrations. This opens up possibilities for new types of gradient experiments, where paracrine signaling can be minimized.

II. MATERIALS AND METHODS

A. Design principle

The design principle used to generate stepwise concentrations was similar to previously reported.[20,21] The experimental reagent and the dilutant were introduced from individual inlets and delivered to eight mixing chambers, as shown in Fig. 1(a). Each of the chambers covered an area of four microwells. In principle, the reagent and dilutant concentrations in the mixing chamber were dependent on the width and length of the flow channels, i.e., microchannel resistances, generating eight steps of logarithmic (100%, 10%, 1%, and 0.1%) and linear (50%, 20%, 5%, and 2%) concentrations.

Assuming Hargen-Poiseuille flow in a rectangular channel and using Ohm's law, the microchannel resistance to the kth chamber, R_k, was expressed as

$$Rk = \frac{8\mu L_{k\_main}(w_{main} + d)^2}{{w_{main}}^3 d^3} + \frac{8\mu L_{k\_daughter}(w_{k\_daughter} + d)^2}{{w_{k\_daughter}}^3 d^3}, \quad (1)$$

A

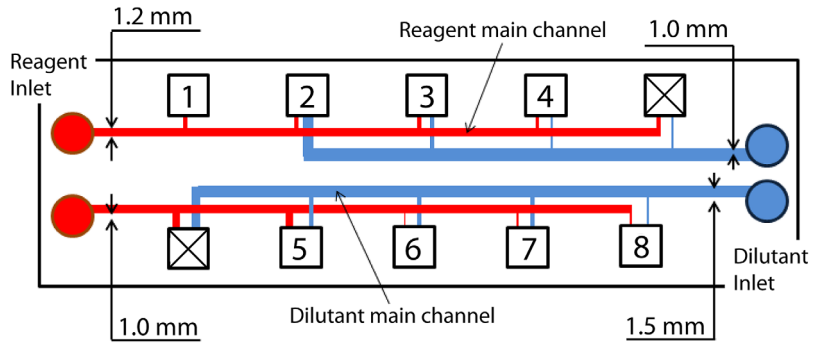

B

Chamber no.		1	2	3	4	X	X	5	6	7	8
Concentration (%)		100	50	20	10	-	-	5	2	1	0.1
Reagent channel	Width (μm)	115	100	66	47	800	695	63	68	89	30
	Length (mm)	8.46	18.93	29.4	39.87	50.34	8.46	18.93	29.4	39.87	50.34
Dilutant channel	Width (μm)	-	1000	193	114	49	100	188	168	113	85
	Length (mm)	50.27	39.81	29.34	18.87	8.41	50.27	39.81	29.34	18.87	8.41

C

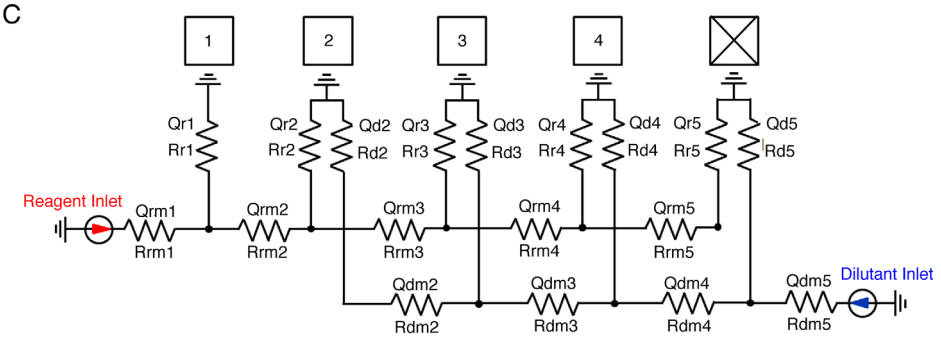

FIG. 1. (a) Specification of the microchannels and numbers of mixing chambers on the device. There were eight mixing chambers and two chambers used to adjust the flow rate (marked with a cross). The reagent channel (red) was in the top layer, whereas the dilution channel (blue) was in the second layer. (b) The width and length of the reagent and dilutant daughter channels. (c) Schematic of the microfluidic resistance network, analogous to an electric circuit.

where μ is the coefficient of viscosity, L_{k_main} is the length of the main microchannel, d is the height of the microchannel, w_{main} is the width of the main microchannel, L_{k_daughter} is the length of the daughter microchannel, and w_{k_daughter} is the width of the daughter microchannel, as shown in Fig. 1(b). The concentration at the kth chamber, C_k, was defined as

$$C_k = \frac{Q_{r_k}}{Q_{r_k} + Q_{d_k}}, \tag{2}$$

where Q_{rk} is the flow rate of the reagent solution and Q_{dk} is the flow rate of the dilutant solution. To determine the required dimensions of the microchannels, the ratio of the flow rates was expressed as a ratio of the microchannel resistance as follows (Eqs. (3)–(8)). First, the microchannel resistance was represented by an electric circuit, as shown in Fig. 1(c). With respect to the reagent solution (chamber 1 to X), the flow rate for $k = 1 - (N - 2)$ was expressed as

$$Q_{r_k} = \frac{R_{rm_{k+1}} + R_{r_{k+1\sim N}}}{R_{r_k}} \times Q_{rm_{k+1}}. \tag{3}$$

For $k = N$,

$$Q_{r_N} = \frac{R_{r_{N-1}}}{\mathrm{R}_{rm_N} + R_{r_N}} \times Q_{r_{N-1}}. \tag{4}$$

Similarly, with respect to the dilutant solution, the flow rate for $K = 3 - N$ was expressed as

$$Q_{d_k} = \frac{R_{dm_{k-1}} + R_{d_{2\sim k-1}}}{R_{d_k}} \times Q_{rd_{k-1}}. \tag{5}$$

For $k = 2$,

$$Q_{d_2} = \frac{R_{d_3}}{R_{dm_2} + R_{d_2}} \times Q_{d_3}. \tag{6}$$

The following relationships for the flow rate were also obtained, for the reagent solution:

$$Q_{r_{m_k}} = Q_{r_k} + Q_{r_{m_{k+1}}}; \quad Q_{r_N} = Q_{r_{m_N}}, \tag{7}$$

and the dilutant solution

$$Q_{d_{m_k}} = Q_{d_k} + Q_{d_{m_{k-1}}}; \quad Q_{d_2} = Q_{d_{m_2}}. \tag{8}$$

B. Characterization of flow in the mixing chamber

CFD was performed to identify a suitable design for the reaction chamber that allowed mixing of the reagent and dilutant solution. A finite element model was constructed using 52 346 three-dimensional tetrahedral finite elements (Fig. 2(a)). In the model, reagent and dilutant solutions were mixed in the reaction chamber to obtain a certain concentration of the reagent (Fig. 2(b)). Colors were used to depict different concentrations; red and blue represented 100% and 0% reagent concentrations, respectively, whereas mixing red and blue inputs generated the color green.

The flow field was assumed to be laminar and at steady-state, and the fluid was assumed to be viscous. The molar mass and density were 46.07 kg/mol and 789 kg/m^3, respectively, for the reagent solution, and 18.02 kg/mol and 997 kg/m^3, respectively, for the dilutant solution. A flow of 3.3 mm/s was applied to the inlet region for both solutions, while the outlet regions were kept unpressurized (at atmospheric pressure). The diffusion coefficient was 10^{-9} m^2/s. A

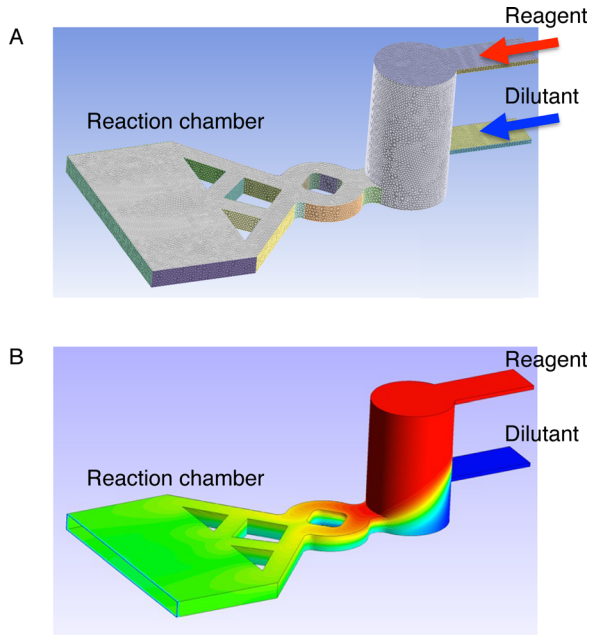

FIG. 2. (a) Finite element model used in the CFD simulations, showing the mixing of reagent and dilutant in a reaction chamber. (b) Results of the CFD analysis in one of the chambers. Mixing of the reagent (red) and dilutant (blue) resulted in a homogeneous solution (green) prior to entering the chamber.

no-slip condition was assumed at all the boundaries. The CFD analysis was conducted using the ANSYS 14.3 commercial code (ANSYS, USA).

C. Device layout

A total of four inlets connected to microchannels (two for the reagent and two for the dilutant) were created on the top layer of the device. Ten outlets were created on the 2nd and 3rd layer, which were connected to the reaction chambers on the 1st layer, enabling draining of the sample. The widths of the two reagent channels were 1000 and 1200 μm, whereas those of the dilutant channels were 1000 and 1500 μm. The height of all channels was 50 μm. The four main channels (reagent and dilutant) were kept separated from the microwell slide by the 1st layer. The experimental reagent and dilutant were introduced from separate inlets and delivered to ten mixing chambers, as shown in Fig. 3(a). Each main microchannel branched into five subsidiary microchannels, one of which was set aside for adjusting the flow rate in the other four microchannels, and thus was not used for the experiment described below. Microchannels for the reagent and dilutant were merged in pairs at ten mixing ports, where the two solutions were mixed by passing them through a mixing lane, prior to entering a chamber. The mixing ports and the mixing lanes were kept separated from the microwell slide to facilitate simple mixing. Different concentrations were achieved by adjusting the volumetric flow rate of each microchannel. The mixing chambers were designed to cover four microwells, and, therefore, cells in those microwells were exposed to the same concentration of reagent. Each chamber had a separate outlet. The flow could, if desired, be stopped shortly after the device is filled, minimizing the dead volume to only encompass microchannels, inlet and outlet tubing. The reagent and dilutant concentrations in the mixing chambers were dependent on the width and length of the flow channels, resulting in an eight step reagent concentration gradient that ranged over three orders of magnitude from $\times 1$ (input concentration) to $\times 0.01$.

D. Microfabrication

The device consisted of a microwell slide integrated with PDMS (polydimethylsiloxane, Sylgard 184, Dow Corning, MI, USA) microfluidic components. The microfluidic components

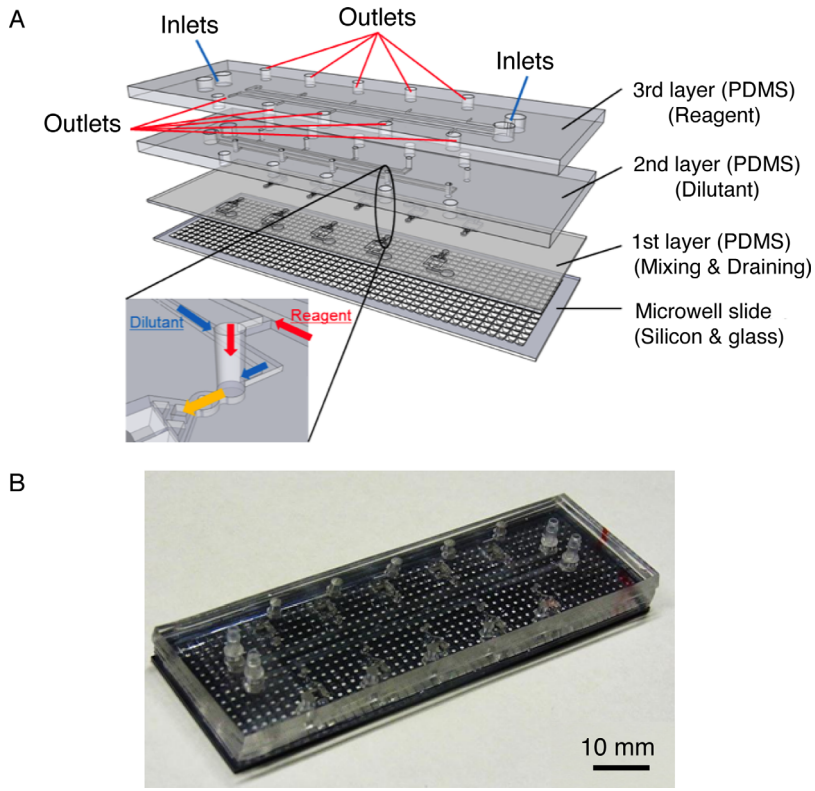

FIG. 3. (a) Schematic of the four layers of the microfluidic device. The reagents were introduced into the channels on the top layer, and the dilutants were introduced into the channels on the second layer. The two solutions were merged before entering the reaction chamber. (b) Photograph of the device with the three PDMS layers bonded to the microwell slide.

allowed desired concentrations of reagents to reach the cells cultured in the microwells. Three microfluidic layers were fabricated using standard silicon-based soft-lithography and a PDMS replica molding technique. The 1st layer was designed to hold the reagent solution, the 2nd layer designed for dilutant solution, and the 3rd layer for mixing/draining of the reagent-dilutant solution. Briefly, silicon wafers were coated with a double stack of 50 μm thick dry resist film (Hitachi Chemical, Tokyo, Japan), using a soft rubber roller on a thermal block. Each coated wafer was exposed to ultra violet light through designated photomasks to construct separate molds for the three layers. The resulting wafers were developed in 1% aqueous solution of sodium carbonate (Wako, Tokyo, Japan). A 10:1 v/v mixture of PDMS polymer and cross-linker (Sylgard 184, Dow Corning Corp., MI, USA) was poured onto the resist molds and cured at 110 °C for 10 min. Thin layers of PDMS were carefully removed from the three molds and then combined under pressure at 100 °C. The two inlets for the dilutant and the ten outlets on the 3rd layer were vertically interconnected to the microchannels and the outlets on the 2nd layer. The mixing ports run through all three layers and were vertically interconnected throughout the structure. This was followed by surface treatment with air plasma (Electro-Technic Products Inc. IL, USA). The combined three layers were then integrated with the microwell slide using plasma bonding.

E. Integration of the microwell slide and microfluidic stepwise concentration generator

The microwell slide consisted of a 500 μm thick, 75 mm $\times$ 25 mm silicon wafer with an array of 672 (14 $\times$ 48) microwells bonded to a 175 μm thick glass slide, which was optimal for high-resolution imaging (Fig. 4). Each well could hold 500 nl of fluid, had tapered sides and measured 650 μm $\times$ 650 μm at the bottom and 1360 μm $\times$ 1360 μm at the top.

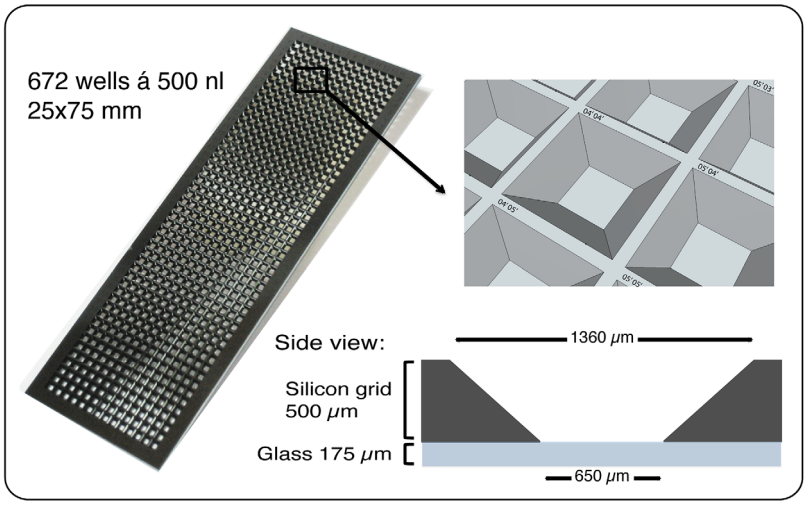

FIG. 4. Photograph of the microwell slide with 672 wells that can each hold 500 nl. It was fabricated from a silicon grid supported on a thin glass slide to facilitate high-resolution imaging. The microwells had tilted walls and are labeled with *x*, *y* coordinates.

As mentioned earlier, the PDMS microfluidic components consisted of three layers: A microchannel layer for reagent solution, a microchannel layer for dilutant solution, and a mixing chamber/drain layer (Fig. 3(a)). Each layer was fabricated individually by photolithography and soft-lithography techniques, using a double stack of an 112 μm thick sheet of dry resist film, and was bound together with the microwell slide on a hotplate, following surface treatment with air plasma (Fig. 3(b)).

F. Experimental validation

To validate the device, a 0.12 mM solution of fluorescein isothiocyanate (FITC)-labeled dextran (30 kDa, Invitrogen, USA) in ultrapure water (reagent) and dextran-free ultra pure water (dilutant) was injected at a flow rate of 100 μl/min for 10 min using a syringe pump (KDS Legato 210, KD Scientific, USA). Micrographs of the chambers were captured using a 4× objective lens and an inverted fluorescent microscope (IX81, Olympus, Japan). The fluorescence intensities could be assumed to be linear to the FITC-dextran concentration within the used concentration range.[22] Fluorescence intensities in the mixing chambers were measured and compared to theoretical calculations for Hargen-Poiseuille flow in a rectangular channel, using Ohm's law adjusted for the different channels.

As a biological proof of concept experiment, bovine aortic endothelial cells (BAECs) (Cell Applications, USA) were cultured in the microfluidic device. Cells at an initial concentration of 1.5×10^5 cells/ml were cultured overnight in Dulbecco's modified Eagle's media (DMEM) (Invitrogen, USA), supplemented with 10% fetal bovine serum (FBS) (Invitrogen, USA), under a controlled environment (37 °C, 5% CO_2). To induce cell death, by permeabilizing the cell membrane, cultured cells were exposed to eight predetermined concentration steps of saponin (Sigma, USA) generated from a 1 mg/ml (0.1 w/w%) stock solution over 10 min at a flow rate of 100 μl/min at 37 °C. The eight chambers from 1–8 (100%-0.1% reagent solution) were exposed to 0.1, 0.05, 0.02, 0.01, 0.005, 0.002, 0.001, and 0.0001 w/w% saponin, respectively. Phosphate buffered saline (PBS) (Invitrogen, USA) was used as dilutant agent. A live/dead assay was performed to quantify the effect of saponin on the cells. Briefly, cells were exposed to 5 μM of calcein acetoxymethylester (AM) (Dojindo Laboratories, Japan), which stains live cells green, and 5 μM ethidium homodimer (Invitrogen, USA), which stains dead cells red, for 20 min. The effect of the live/dead stain was monitored using an inverted fluorescent microscope (IX81, Olympus; Japan) and the experiment was repeated for four replicates.

III. RESULTS AND DISCUSSION

Microfluidic devices enable addition of fluids/reagents to designated areas in a controlled way, which is unparalleled by open culture systems. By performing cell experiments in a closed system, with isolated locations, problems, such as interference by intercellular paracrine signaling from cells in neighboring areas, are eliminated. In developing the described device, we took advantage of the compartmentalized structure of a previously developed microwell slide and integrated it with a microfluidic system, where the microfluidic channel dimensions governed the concentration of fluid that reached eight different chambers.

Flow simulations were carried out to visualize the theoretical fluid profile in the chambers. The CFD analysis indicated that the reagent solution (depicted in red) and dilutant solution (in blue) were fully mixed prior to entering the reaction chambers (Fig. 2(b)). In this figure, 100% and 0% reagent concentrations are shown as red and blue, respectively, whereas mixing of the reagent and dilutant is illustrated in green.

To test if the theoretical calculations were correct, proof of concept experiments was performed. The microfluidic device was validated by injecting FITC-labeled dextran (reagent) and ultrapure water (dilutant) into the device. The measured fluorescence intensities of the FITC-dextran solution were compared with the theoretical calculations, for each reaction chamber, as shown in Fig. 5. The experimental fluorescence intensities were normalized by the intensity measured in reaction chamber 1. It was confirmed that eight stepwise concentrations of the FITC-dextran solution were generated, spanning three orders of magnitude, and that the experimental results were in accordance with the theoretical calculations. However, there were some minor discrepancies between the experimental and theoretical data at low concentrations, which may be due to fabrication errors of the microchannels or be due to a pump related issue. Microchambers 1–4 and 5–8 are connected to two separate micropumps. It is also possible that particles or dust was caught in the device, influencing the mixing process or creating an irregular flow, resulting in slight intensity variations between the chambers.

After establishing the functionality of the stepwise concentration generator, the device's biological compatibility was tested by performing a cytotoxicity assay on BAECs cultured in the device and then subjected to various concentrations of saponin. Fig. 6 shows representative fluorescent images of the eight mixing chambers after exposure to saponin solution. In the cases of 0.1 w/w% and 0.05 w/w% saponin solution, all cells appeared to be dead (red). Starting from 0.02 w/w% saponin solution, the number of live cells (green) increased with decreasing concentration of saponin, while the number of dead cells decreased. For 0.0001 w/w% saponin

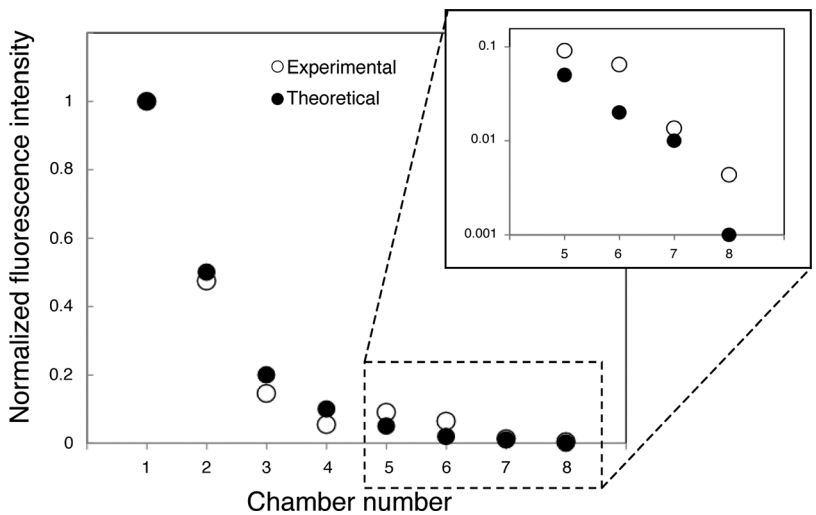

FIG. 5. Comparison of the experimental results (open circles) with the theoretical calculations (closed circles) in the eight mixing chambers, after flowing FITC-dextran labeled ultrapure water (reagent) and ultrapure water (dilutant) through the device. The data were normalized to fluorescence intensity recorded in chamber 1.

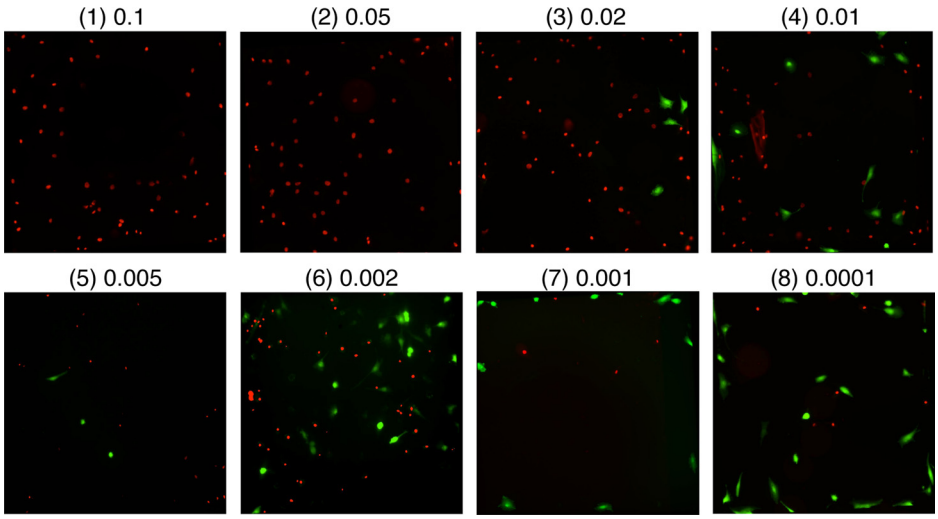

FIG. 6. Fluorescent micrographs showing a representative chamber for each of the eight concentration steps: Chamber 1 (0.1 w/w% saponin) to chamber 8 (0.0001 w/w% saponin). The cells were stained with a live (green, calcein AM)/dead (red, ethidium homodimer) stain to quantify the effect of saponin on the cells.

solution, most cells were alive. Fluorescent images were captured for four replicates and quantitatively analyzed to determine the percentage of live cells, which clearly increased as the concentration of saponin solution decreased from 0.02 w/w% down to 0.0001 w/w% (Fig. 7). Saponin's toxicity effect in the present device is in the same concentration range as traditional toxicity assays.[23] The results showed that the presented microfluidic device allows designated concentration steps of a reagent to be generated in different chambers, adding an important functionality to the microwell slide.

The proposed microfluidic stepwise concentration generator has several advantages, compared to previously reported devices. First, the stepwise concentrations in the present device are generated by a simple microchannel configuration. Previous studies have reported designs based on ladder networks, which rely on complex microchannel systems to create a wide range of concentrations.[20,24] In contrast, the present device can create various microchannel resistances by tuning both the width and length of the microchannels, which enables a configuration with a simple microchannel branching network. Second, to reduce the microfluidic resistance, the

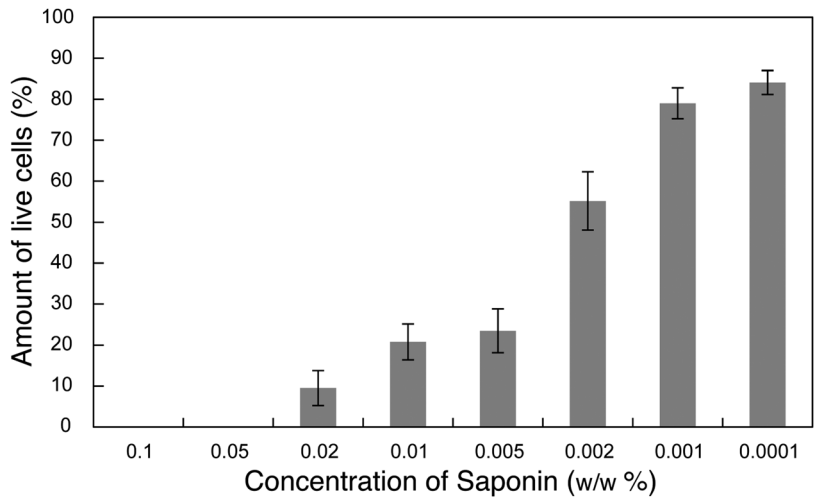

FIG. 7. Percentage of live cells after exposure to eight concentration steps of saponin. The data are expressed as mean ± SD and are based on four replicates.

mixer was designed, so that the reagent and dilutant travel through a branch-like configuration that is sufficiently long to allow proper mixing before reaching the main reservoir. Third, with regard to dimension, the proposed device was based on a microwell slide that was the same size as a commercially available microscope slide. This makes the device easy to transfer to other platforms for real-time data acquisition or various readout techniques. Cells could be cultivated in the microwells and then selectively subjected to loaded reagents, drugs, etc. The microchannel networks in the PDMS layers could be designed to generate a different set of serial dilutions or to utilize other groups of microwells on the slide, etc. Thus, the proposed device offers a versatile stepwise concentration generator that can support various extended applications.

We believe that this device has many potential applications for generating various concentration gradients on a miniature scale, minimizing the amount of biological sample and reagents required, compared to devices on the macro scale. One example could be cytotoxicity assays, e.g., screening for different cytostatics or antibiotics. Another application could be to program/reprogram stem/differentiated cells, by subjecting them to various amounts of transcription factors to find new relevant factors and conditions.[25] The device could be developed for use in high content heterogeneity studies, where clonal expansion from single cells is monitored and exposed to different reagent concentrations.

IV. CONCLUSIONS

Here, we presented a simple microchannel configuration that enables cells to be subjected to a stepwise concentration gradient, using the compartmentalized structure of a microwell slide. The microchannel configuration was designed using electrical circuit analogy. Theoretical characterization of the flow profile was performed using CFD analysis, which showed that the reagent and dilutant were fully mixed prior to entering the cultivation chambers. The device was experimentally verified by injecting an aqueous solution of FITC-labeled dextran. The measured fluorescence intensities were found to be in good agreement with theoretical calculations. In a separate experiment, BAECs were cultured in the chambers and subjected to a concentration gradient of saponin. The results demonstrated the potential of the device, for further biological experiments. The device enables cells to be cultured and analyzed at discrete and isolated locations, eliminating problems associated with paracrine signals from cells subjected to other concentrations.

ACKNOWLEDGMENTS

This work was financially supported by the Grants-in-Aid for Scientific Research (B) program (Grant No. 24300157) from the Ministry of Education, Culture, Sports, Science and Technology (MEXT) of Japan and the strategic Japanese-Swedish cooperative program on "Multidisciplinary BIO" overseen by the Japan Science and Technology Agency (JST), the Swedish Governmental Agency for Innovation Systems (VINNOVA), and the Swedish Foundation for Strategic Research (SSF).

[1]T. M. Keenan and A. Folch, Lab Chip **8**, 34 (2008).
[2]S. Boyden, J. Exp. Med. **115**, 453 (1962).
[3]S. H. Zigmond, J. Cell Biol. **75**, 606 (1977).
[4]E. F. Foxman, J. J. Campbell, and E. C. Butcher, J. Cell Biol. **139**, 1349 (1997).
[5]R. W. Gundersen and J. N. Barrett, Science **206**, 1079 (1979).
[6]B. G. Chung and J. Choo, Electrophoresis **31**, 3014 (2010).
[7]G. M. Walker, M. S. Ozers, and D. J. Beebe, Sens. Actuators, B **98**, 347 (2004).
[8]S.-Y. Cheng, S. Heilman, M. Wasserman, S. Archer, M. L. Shuler, and M. Wu, Lab Chip **7**, 763 (2007).
[9]J. Diao, L. Young, S. Kim, E. A. Fogarty, S. M. Heilman, P. Zhou, M. L. Shuler, M. Wu, and M. P. DeLisa, Lab Chip **6**, 381 (2006).
[10]N. L. Jeon, S. K. W. Dertinger, D. T. Chiu, I. S. Choi, A. D. Stroock, and G. M. Whitesides, Langmuir **16**, 8311 (2000).
[11]D. Irimia, D. A. Geba, and M. Toner, Anal. Chem. **78**, 3472 (2006).
[12]K. W. Oh, K. Lee, B. Ahn, and E. P. Furlani, Lab Chip **12**, 515 (2012).
[13]W. Dai, Y. Zheng, K. Q. Luo, and H. Wu, Biomicrofluidics **4**, 024101 (2010).
[14]C.-W. Wei, J.-Y. Cheng, and T.-H. Young, Biomed. Microdevices **8**, 65 (2006).

[15]S. Lindström and H. Andersson-Svahn, Biochim. Biophys. Acta **1810**, 308 (2011).
[16]S. Lindström, R. Larsson, and H. Andersson-Svahn, Electrophoresis **29**, 1219 (2008).
[17]S. Lindström, M. Eriksson, T. Vazin, J. Sandberg, J. Lundeberg, J. Frisén, and H. Andersson-Svahn, PLoS ONE **4**, e6997 (2009).
[18]S. Lindström, M. Hammond, H. Brismar, H. Andersson-Svahn, and A. Ahmadian, Lab Chip **9**, 3465 (2009).
[19]S. Lindström, K. Mori, T. Ohashi, and H. Andersson-Svahn, Electrophoresis **30**, 4166 (2009).
[20]C. Kim, K. Lee, J. H. Kim, K. S. Shin, K. J. Lee, T. S. Kim, and J. Y. Kang, Lab Chip **8**, 473 (2008).
[21]M. Yamada, T. Hirano, M. Yasuda, and M. Seki, Lab Chip **6**, 179 (2006).
[22]S. Y. Yuan and R. R. Rigor, *Regulation of Endothelial Barrier Function* (Morgan & Claypool Publishers, 2010), Chap III, p. 5.
[23]Z. Wang, M.-C. Kim, M. Marquez, and T. Thorsen, Lab Chip **7**, 740 (2007).
[24]S. Sugiura, K. Hattori, and T. Kanamori, Anal. Chem. **82**, 8278 (2010).
[25]S. Liebau, P. U. Mahaddalkar, H. A. Kestler, A. Illing, T. Seufferlein, and A. Kleger, Stem Cells Dev. **22**, 695 (2013).